Macromolecular Research, Vol. 16, No. 5, pp 399-403 (2008)

Monodisperse Micrometer-Ranged Poly(methyl methacrylate) Hybrid Particles Coated with a Uniform Silica Layer

Seung-Jin Han, Kyomin Shin, and Kyung-Do Suh*

Division of Chemical Engineering, College of Engineering, Hanyang University, Seoul 133-791, Korea

Jee-Hyun Ryu

Display Materials Team (CR), Cheil Industries Inc., 332-2, Gocheon-dong, Uiwang-si, Gyeonggi-do 437-711, Korea

Received September 3, 2007; Revised February 14, 2008; Accepted February 23, 2008

Abstract: Monodisperse, micron-sized, hybrid particles having a core-shell structure were prepared by coating the surface of poly(methyl methacrylate)(PMMA) microspheres with silica and by copolymerizing acrylamide (AAm) to supply the hydrogen bonding effect by means of the amide groups. Tetraethoxysilane (TEOS) was then slowly dropped onto the medium under certain conditions. Because of the hydrogen bonding between the amide of the PMMA particles and the hydroxyl group of the hydrolyzed silanol, a silica shell was generated on the PMMA core particles. The morphology of the hybrid particles was investigated with transmission (TEM) and scanning (SEM) electron microscopy as a function of the medium conditions and the amount of TEOS. Improved thermal properties were observed by TGA analysis.

Keywords: sol-gel process, hybrid particles, hydrogen bonding, silica shell, thermal property.

Introduction

Organic-inorganic composite materials have been the subject of intense investigations due to the possibility of the improvement of colloidal properties. Additional thermal, mechanical, electrical, and optical properties can be efficiently incorporated into the polymer particles utilizing a hybrid technique.[1-4] A sol-gel process has been commonly employed in the preparation of the hybrid composites since it can be carried out simply and rapidly at low temperatures and mild conditions.[5,6] By applying the sol-gel process, various preparation methods such as layer-by-layer deposition,[7] surface modification[8] by functional groups, and a spray drying method,[9] have been reported along with different morphologies such as core-shell,[10] hollow,[11] and raspberry.[12]

In a recent study, hybrids coated with silica on the polymer surface via surface modification have been reported.[13,14] The most important route of surface modification is by a covalent bonding method[16,17] and, more specifically, by a charge interaction method.[18-20] The silica particles produced by the Stöber process generally have a negative charge, which can be easily coated on the surface of positively charged polymer particles. Most of the hybrid composites, however, had much rough and/or mesoporous shell on the surface because of difficulty in controlling the uniformity and thickness of the silica shell.[21-23]

In the present study, to control the uniformity and thickness of the silica shell, we incorporated functional group on the particles surface. We produced highly monodispersed organic-inorganic hybrid microspheres having uniform silica shell on the surface. The hydrogen bonding moiety was incorporated into the PMMA particles by copolymerizing of methylmethacrylate and acrylamide for efficient sol-gel processing. The morphology and the surface of the hybrid micron-sized particles were observed by scanning and transmission electron microscopy, respectively. The silica surface layer on the particles was investigated as a function of the medium composition ratios and tetraethoxysilane (TEOS) content. The thickness of the silica layer was also measured. Finally, the thermal stability of the hybrid microspheres was examined utilizing thermogravimetric analysis.

Experimental

Materials. Methyl methacrylate (MMA, Junsei) and acrylamide (AAm, Aldrich) were used to obtain the amide-functionalized PMMA particles. 2,2′-Azobis(isobutyronitrile) (AIBN, Junsei) was recrystallized from methanol before using. Poly(vinyl pyrrolidone)(PVP, $M_w = 4.0\times10^4$ g/mol, Aldrich), aerosol-OT (AOT, Wako), tetraethoxysilane (TEOS, 99.9%,

*Corresponding Author. E-mail: kdsuh@hanyang.ac.kr

Table I. Conditions and Characterization of the Hybrid Particles[a]

Experiment No.	Substrate[b] (g)	TEOS (g)	Methanol (g)	DDI[c] (g)	NH_4OH (mL)	Silica Layer
1	0.5	3.5	18.0	2.0	0.7	Cracked
2	0.5	3.5	17.0	3.0	0.7	Incomplete
3	0.5	3.5	14.0	6.0	0.7	80-100 nm
4	0.5	1.5	14.0	6.0	0.7	40 nm
5	0.5	5.0	14.0	6.0	0.7	160-200 nm

[a]Sol-gel process condition: room temperature for 12 h. [b]P(MMA-*co*-AAm) particles. [c]Distilled deionized water.

Aldrich), ammonia water (25~28%, Yakuri), methanol (J. T. Baker), and distilled deionized (DDI) water were used without further purification.

Preparation of Poly(MMA-*co*-AAm) Microsphere and Sol-Gel Process. Firstly, the micron-sized poly(MMA-*co*-AAm) particles were produced by dispersion polymerization using acrylamide as comonomer following the process of the literature.[24] Then, the silica coated hybrid particles were directly obtained by a sol-gel process. Amide functionalized poly(MMA-*co*-AAm) particles (0.5 g) were redispersed in a solution of methanol and water in a bottom-bottom flask. To ascertain the medium effect in the sol-gel process, the methanol/water ratio of the medium was varied. After ultrasonication for 10 min, seeds were perfectly dispersed in the medium and 0.7 mL of an ammonia solution (25-28%) as catalyst was added until the pH was about 11.2. To obtain hybrid particles with different shell thicknesses, various amounts of TEOS were slowly dropped onto the medium in the reactor. This reaction was maintained for 12 h at room temperature under constant stirring. Finally, the hybrid particles were repeatedly centrifuged by deionized water at 1,000 rpm and dried in a vacuum oven.

Characterizations. The amide groups of poly(MMA-*co*-AAm) particles and silica gel on the surface of hybrid particles were confirmed by FT-IR (Nicolet, Mahgna IR-550). To confirm the presence of the coated silica layer and thermal stability of the particles, thermogravimetric analysis (TGA) operating at a heating rate of 10 °C/min in the range 0-1,000 °C was conducted. The surface morphology of seed and hybrid particle were observed with a scanning electron microscope (SEM, JSM-6300, JEOL). The morphology and shell thickness were examined with a transmission electron microscope (TEM, Cal Zeiss LIBRA 120).

Results and Discussion

Linear PMMA and poly(MMA-*co*-AAm) produced by dispersion polymerization were composed of highly monodisperse micron-size particles with an average diameter of 3.366 and 3.981 μm, respectively (Figure 1). Above 3 wt% of amide contents, poly(MMA-*co*-AAm) particles had polydisperse size distribution. Hence, the acrylamide content

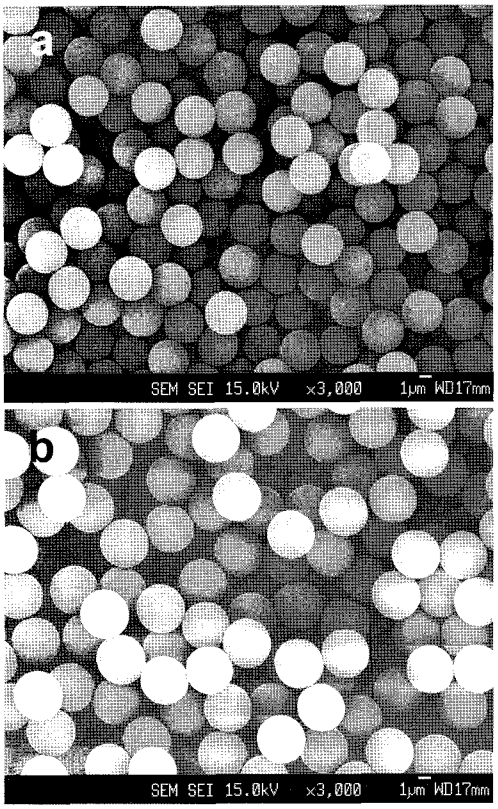

Figure 1. SEM images for (a) linear PMMA and (b) poly(MMA-*co*-AAM) particles.

was fixed at 3 wt% to maintain monodispersity in our system and the incorporated amide group was confirmed by the FT-IR spectrum (Figure 2(b)). The characteristic bands of the amide group were clearly observed in copolymer particles with the N-H stretch occurring at around 3300 cm^{-1}. This shows that poly(MMA-*co*-AAm) was successfully prepared by the co-polymerization system.

By the hydrogen bonding interaction, the silica sols were coated directly on the surface of the amide group incorporated PMMA. The functionalized PMMA particles had a ξ-potential of +1.63 mV and silica the particles had a ξ-potential of -24.7 mV at a pH 11.2. After coating with silica, the hybrid particles had a negative charge of about -7.3 mV

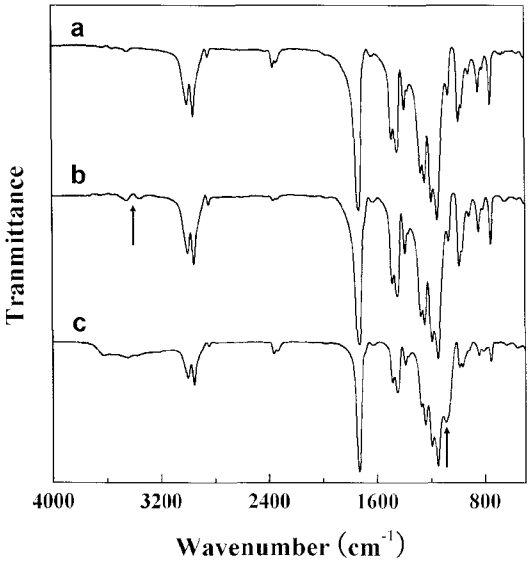

Figure 2. FT-IR spectra for (a) PMMA, (b) poly(MMA-*co*-AAM) particles, and (c) poly(MMA-*co*-AAM)-silica hybrid particles.

Table II. Characterization of PMMA and Poly(MMA-*co*-AAM) Hybrid Microspheres

Sample[a]	Particle Sizes[b] (μm)		PDI[c]	CV[d]
	D_n	D_w		
PMMA	3.366	3.368	1.0007	1.61
Poly(MMA-*co*-AAM)	3.981	3.982	1.0003	0.92
Experiment No. 3	4.156	4.158	1.001	1.34
Experiment No. 4	4.062	4.063	1.001	1.29
Experiment No. 5	4.387	4.389	1.001	1.37

[a]Samples correspond with TEOS ratio based on the weight of sub strate as shown in Table I.
[b]Average particle diameter, $D_n = \Sigma(D_i/N)$, $D_w = \Sigma D_i^4 / D_i^3$.
[c]Particle size distribution, D_w/D_n.
[d]Coefficient variation, $CV(\%) = \sigma/D_n \times 100$, where σ is standard deviation.

on the surface. This indicates that silica sol was successfully coated on the PMMA particles by the sol-gel process. The coated silica layer was also observed by the FT-IR spectrum. The characteristic bands of silica were clearly observed in hybrid particles with the Si stretch occurring at around 1000-1100 cm^{-1} (Figure 2(c)).

We also utilized a transmission electron microscope (TEM) to confirm the effect of varying the acrylamide content in the silica coating process. The pure PMMA and poly (MMA-*co*-AAm) particles underwent the sol-gel process with identical conditions (see experiment no. 3 in Table I). As a result, the pure PMMA did not have a uniform silica layer on the surface; silica was partially coated or not. On the other hand, amide group modified poly(MMA-*co*-AAm) particles were coated with a silica layer by hydrogen bonding interaction (Figure 3). This means that the hydrogen bonding effect of acrylamide was a critical factor for silica coating during the sol-gel process. This is the result of hydrogen bonding attraction between amide group and hydrolyzed silanol precursor of TEOS.[15]

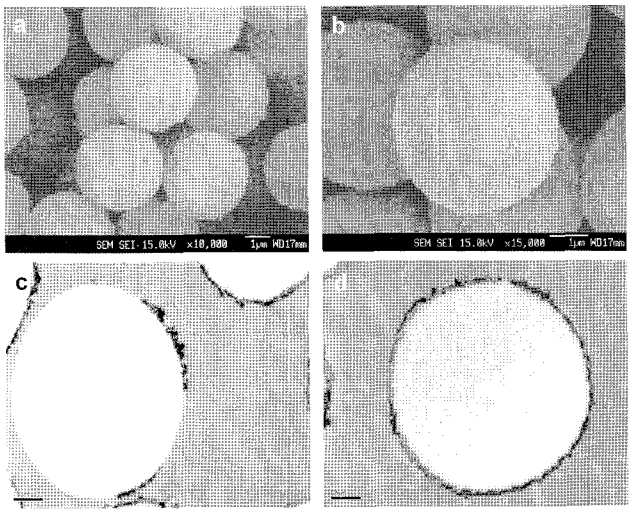

Figure 3. SEM and TEM images of pure, (a) and (c); and amide-functionalized, (b) and (d) PMMA-silica hybrid particles.

In the sol-gel process, the ratio of H_2O/TEOS, the R value, strongly affects the reaction rate. When the R value is increased in the sol-gel system, the hydrolysis reaction rate increases and hydrolysis of monomers occurs more readily. Similarly, the water ratio increased in the medium, and the coating of silica on the PMMA particles occurred more perfectly and strongly in our system. The water/medium ratio was changed in the range of 10-30% (experiment no. 1, 2, 3). As shown in Figure 3, the morphology of hybrid particles changed depending on the different water ratio. At a 10% water ratio, cracked morphology of the silica layer was observed because of thinness and weak cohesion (Figure 4(a)). For the 15% ratio, although the silica was coated incompletely, a more stable silica layer was generated on the surface (Figure 4(b)). The most uniform silica layer coated hybrid particles were produced at a 30% water ratio (Figure 4(c)). Above a 30% water/medium ratio, however, the sol-gel reaction did not proceed well. At high water ratios, a decrease of TEOS solubility slowed down the sol-gel reaction rate and the gel-reaction time became longer due to low hydrolysis and condensation rates.

The shell thickness of silica on the hybrid particles was affected by several factors such as pH value, temperature, type of catalyst, and reaction time. In particular, TEOS concentration directly affected the silica thickness in the sol-gel process. In the present study, the silica layer thickness increased in proportion to TEOS concentration in the sol-gel process. The change of shell thickness was examined through TEM images (Figure 5) when the dropped TEOS

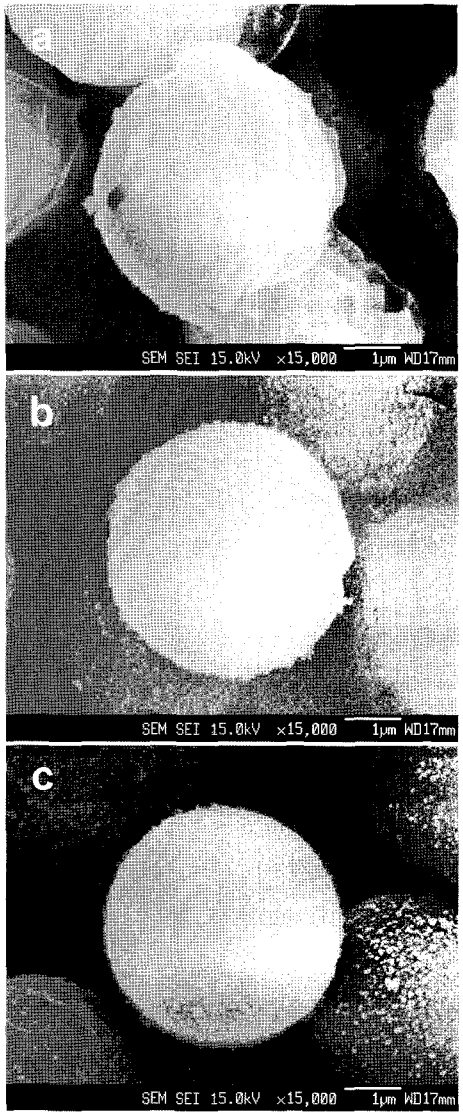

Figure 4. SEM images of PMMA-silica hybrid particles with water ratios in the medium of (a) 10 wt%, (b) 15 wt%, and (c) 30 wt%.

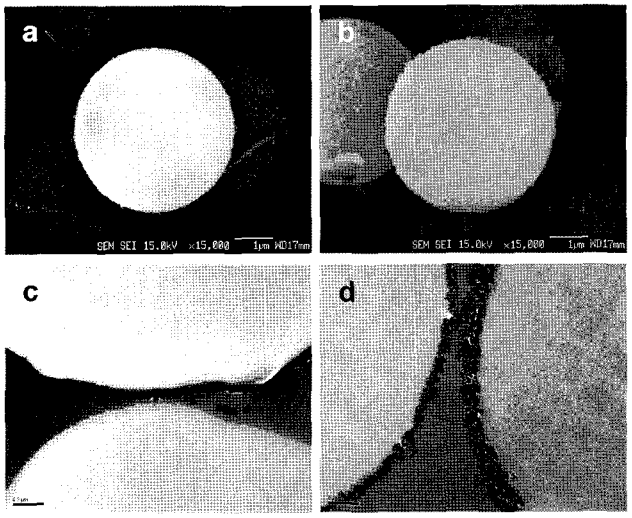

Figure 5. SEM and TEM images of PMMA-silica hybrid particles at 3-fold TEOS content, (a) and (c); and 10-fold TEOS content, (b) and (d).

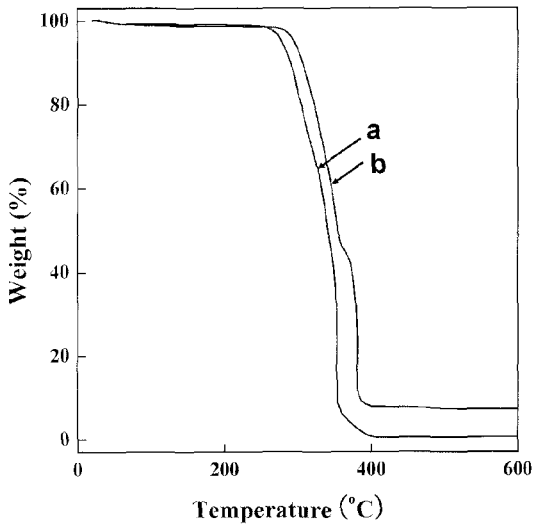

Figure 6. TGA thermograms of (a) PMMA and (b) PMMA-silica hybrid particles.

volume was changed by 3- to 10-fold (experiment no. 1, 4, 5). As a result, the shell thickness of silica increased from 40 to 200 nm and the silica layer was uniformly coated on the PMMA particles in the entire range (Figures 5(c), 5(d)). However, the generated silica shells were not thicker than 200 nm when using above a 10-fold increase. The particles had a rough, non-uniform surface although the silica layer had a thickness greater than 400 nm. Excess TEOS formed secondary nano-silica particles in the medium which were adsorbed on the surface of the hybrid particles.

TGA analysis was carried out up to 800 °C at a rate of 10 °C/min under N_2 atmosphere to confirm the improved thermal properties of PMMA-silica hybrid particles. Figure 6 shows the TGA thermogram for the linear PMMA particles and silica coated hybrid particles. It was observed that the thermal stability of the hybrid particles was improved by the silica layer, even though it was about 200 nm thick. The thermal decomposition of the linear PMMA and hybrid particles appeared above 240 °C and 265 °C, respectively. The degradation temperature of hybrid particles was 380.2 °C and that of the pure PMMA particles was 352.6 °C. The silica content of the hybrid particles determined from calculation of the residual weight in the thermogram curves was 6.86% at 800 °C. In accordance with this result, although the silica thickness was about 200 nm, the thermal stability of polymer particles can be improved by thickness control of silica layer.

Conclusions

In this study, we produced monodisperse micron-sized organic-inorganic hybrid particles through dispersion polymerization and a sol-gel process. This process was simple and successfully resulted in a uniform and strongly coated silica layer on the particle surface. It was observed that the ratio of water/medium and TEOS concentration had influences on the morphology of the coated silica layer. The thermal properties of hybrid particles were improved by the coated silica layer. This fact was confirmed through TGA analysis. TGA measurements on the hybrid particles show that the PMMA/silica composite microspheres can maintain improved thermal stability.

Acknowledgement. This work was supported by The Generic Technology Development Program, Ministry of Commerce, Industry and Energy, Republic of Korea (Grant Number: 10021149).

References

(1) Y. Zhao and D. A. Schiraldi, *Polymer*, **46**, 11640 (2005).
(2) A. Samokhvalov, R.W. Gurney, M. Lahav, and R. Naaman, *J. Phys. Chem. B*, **106**, 9070 (2002).
(3) X. P. Zhao and X. Duan, *J. Colloid Interface Sci.*, **251**, 376 (2002).
(4) F. Mammeria, L. Rozesa, E. L. Bourhisb, and C. Sanchez, *J. Eur. Ceram. Soc.*, **26**, 267 (2006).
(5) W. Stober, A. Fink, and E. Bohn, *J. Colloid Interface Sci.*, **26**, 62 (1968).
(6) K. S. Rao, K. El-Hami, T. Kodaki, K. Matsushige, and K. Makino, *J. Colloid Interface Sci.*, **289**, 125 (2005).
(7) F. Caruso, *Adv. Mater.*, **13**, 11 (2001).
(8) I. Tiossot, C. Novat, F. Lefebvre, and E. Bourgeat-Lami, *Macromolecules*, **34**, 5737 (2001).
(9) F. Iskandar, Mikrajuddin, and K. Okuyama, *Nano Letters*, **1**, 231 (2001).
(10) M. Chen, S. Zhou, L. Wu, S. Xie, and Y. Chen, *Macromol. Chem. Phys.*, **206**, 1896 (2005).
(11) A. Imhof, *Langmuir*, **17**, 3579 (2001).
(12) J. Luna-Xavier, A. Guyot, and E. Bourgeat-Lami, *Polym. Int.*, **53**, 609 (2004).
(13) J. H. Moon, W. McDaniel, and Lawrence F. Hancock, *J. Colloid Interface Sci.*, **300**, 117 (2006).
(14) Y. Y. Sun, Z. Zhang, and C. P. Wong, *J. Colloid Interface Sci.*, **292**, 436 (2005).
(15) J. S. Jang and H. S. Park, *J. Appl. Polym. Sci.*, **83**, 1817 (2002).
(16) Michael S. Fleming, Tarun K. Mandal, and David R. Walt, *Chem. Mater.*, **13**, 2210 (2001).
(17) H. Wang, P. Xu, S. Meng, W. Zhong, W. Du, and Q. Du, *Polym. Degrad. Stab.*, **91**, 1455 (2006).
(18) C. Wu, T. Xu, and W. Yang, *Eur. Polym. J.*, **41**, 1901 (2005).
(19) E. Rubio, J. Almaral, R. Ramírez-Bon, V. Castaño, and V. Rodríguez, *Opt. Mater.*, **27**, 1266 (2005).
(20) H. Xiao and N. Cezar, *J. Colloid Interface Sci.*, **267**, 343 (2003).
(21) Y. B. Zhang, X. F. Qian, H. A. Xi, J. Yin, and Z. K. Zhu, *Mater. Lett.*, **58**, 222 (2003).
(22) Y. Lu, J. McLellan, and Y. Xia, *Langmuir*, **20**, 3464 (2004).
(23) N. Kawahashi and E. Matijević, *J. Colloid Interface Sci.*, **138**, 2 (1990).
(24) J. W. Kim and K. D. Suh, *Colloid Polym. Sci.*, **277**, 66 (1999).